INSTITUTE OF PHYSICS PUBLISHING JOURNAL OF PHYSICS: CONDENSED MATTER

J. Phys.: Condens. Matter **17** (2005) 2493–2507 doi:10.1088/0953-8984/17/15/020

Structural phase transition and dielectric relaxation in $Pb(Zn_{1/3}Nb_{2/3})O_3$ single crystals

Y-H Bing[1], A A Bokov[1], Z-G Ye[1,3], B Noheda[2] and G Shirane[2]

[1] Department of Chemistry, Simon Fraser University, 8888 University Drive, Burnaby, BC, V5A 1S6, Canada
[2] Physics Department, Brookhaven National Laboratory, Upton, NY 11973-500, USA

E-mail: zye@sfu.ca

Received 26 January 2005, in final form 26 January 2005
Published 1 April 2005
Online at stacks.iop.org/JPhysCM/17/2493

Abstract

The structure and the dielectric properties of $Pb(Zn_{1/3}Nb_{2/3})O_3$ (PZN) crystal have been investigated by means of high-resolution synchrotron x-ray diffraction (with an x-ray energy of 32 keV) and dielectric spectroscopy (in the frequency range 100 Hz–1 MHz). At high temperatures, the PZN crystal exhibits a cubic symmetry and polar nanoregions inherent to relaxor ferroelectrics are present, as evidenced by the single (222) Bragg peak and by the noticeable tails at the base of the peak. At low temperatures, in addition to the well-known rhombohedral phase, another low-symmetry, probably monoclinic, phase is found. The two phases coexist in the form of mesoscopic domains. The ferroelectric phase transition is diffuse and observed between 325 and 390 K, where the concentration of the low-temperature phases gradually increases and the cubic phase disappears upon cooling. However, no dielectric anomalies can be detected in the temperature range of the diffuse phase transition. The temperature dependence of the dielectric constant shows a maximum at higher temperature (T_m = 417–429 K, depending on frequency) with the typical relaxor dispersion at $T < T_m$ and the frequency dependence of T_m fitted to the Vogel–Fulcher relation. Application of an electric field upon cooling from the cubic phase or poling the crystal in the ferroelectric phase gives rise to a sharp anomaly of the dielectric constant at $T \approx 390$ K and greatly diminishes the dispersion at lower temperatures, but the dielectric relaxation process around T_m remains qualitatively unchanged. The results are discussed in the framework of the present models of relaxors and in comparison with the prototypical relaxor ferroelectric $Pb(Mg_{1/3}Nb_{2/3})O_3$.

(Some figures in this article are in colour only in the electronic version)

[3] Author to whom any correspondence should be addressed.

1. Introduction

$Pb(Zn_{1/3}Nb_{2/3})O_3$ (PZN) and $Pb(Mg_{1/3}Nb_{2/3})O_3$ (PMN) are two prototypical relaxor ferroelectric materials with complex perovskite structure, in which the off-valent Zn^{2+} (or Mg^{2+}) and Nb^{5+} ions occupying the B-sites are primarily disordered [1]. Research on relaxor ferroelectrics and related materials has undergone an accelerated growth in the last few years both in fundamental understanding of the structure and physical properties and in practical applications. This is partly due to the excellent piezoelectric properties discovered in single crystals of the solid solutions between PZN (or PMN) and ferroelectric $PbTiO_3$, which point to the next generation of electromechanical transducer applications [2, 3]. Recent neutron scattering studies have identified a ferroelectric soft mode in PMN at 1100 K that becomes overdamped below the Burns temperature $T_d \approx 620$ K (i.e. the temperature at which polar nanoregions, PNRs, begin to appear), suggesting a direct connection between the soft mode and the PNRs [4]. More interestingly, at lower temperature the soft mode in PMN reappears close to $T_C = 213$ K [5], the temperature at which the electric field-induced polarization vanishes spontaneously upon zero-field heating [6], and a peak in the temperature dependence of the hypersonic damping appears [7]. To interpret the measured intensities of the diffuse scattering in PMN in accordance with the concept of ferroelectric soft mode, Hirota *et al* [8] have proposed and demonstrated the validity of a phase-shifted condensed soft mode model of the PNRs. This model suggests the displacement of PNRs along their polar directions relative to the surrounding cubic matrix (H-shift). Therefore, the phonon dynamics clearly indicates the ferroelectric nature of the relaxor PMN, although the average structure of the system remains cubic and optically isotropic.

Application of an electric field along the $\langle 111 \rangle$ direction can induce a long-range (single domain) ferroelectric phase in PMN, with the development of a polar rhombohedral $R3m$ phase associated with switchable polarization and birefringent macro domains [6, 9, 10].

By means of dielectric spectroscopy, Bokov and Ye [11–13] discovered a 'universal' relaxor dispersion in PMN and related materials, and showed that it is an important common property of relaxor ferroelectrics. The universal relaxor polarization is described by a microscopic model of 'soft' polar nanoregions with unit cells that can freely choose several different directions, while the direction of the total moment of the nanoregion remains the same [13]. Such an approach makes it possible to apply a standard spherical model to relaxor ferroelectrics, which predicts the experimentally observed quadratic divergence of the universal part of the susceptibility above the critical temperature. This model is complementary to the so-called spherical random-bond–random-field model proposed by Blinc *et al* [14, 15] to explain the NMR data and the non-linearity of the total dielectric susceptibility in relaxors.

In comparison with PMN, the crystal structure and polar order of PZN appear to be quite different. Earlier works reported that a phase transition from a cubic to a rhombohedral phase took place upon cooling, which was associated with the maximum of dielectric constant occurring at T_m around 410 K [16–18]. At room temperature weakly birefringent domains with extinction directions along $\langle 110 \rangle_{cub}$ were observed on a $(001)_{cub}$-cut PZN platelet, which seems to confirm the rhombohedral symmetry. The value of birefringence decreases gradually upon heating but more sharply around 390 K before vanishing at $T \geqslant 413$ K [19]. Recently, Lebon *et al* [20] reported that the cubic-to-rhombohedral phase transition in PZN is diffuse and spreads over the temperature range between 385 and 325 K with a full establishment of the rhombohedral phase below 325 K. This phase consists of domains of mesoscopic (60–70 nm) size. Application of a dc field along $\langle 111 \rangle$ transforms the polydomain state into a rhombohedral quasi-monodomain state. High-energy x-ray diffraction studies on PZN crystals by Xu *et al* [21] revealed Bragg peaks resembling a tetragonal (or pseudo-cubic) symmetry (X-phase) for

the bulk crystal, the nature of which is yet to be clarified. On the other hand, neutron scattering results showed the onset of diffuse scattering at the Burns temperature, and a softening of the optical mode at the critical temperature, analogous to PMN [22].

Despite recent intensive work, the nature of phase transitions and dielectric relaxation in relaxors has not been thoroughly understood. In this work, we have studied the structural transformation in PZN crystals by synchrotron x-ray diffraction and by analysing the dielectric properties as a function of temperature and frequency at zero field and under a dc field.

2. Experiment

PZN single crystals were grown by spontaneous nucleation from high-temperature solution according to the method and conditions described in [23]. A crystal plate of triangular shape (4 mm in edge and 330 μm thick) was cut with large surfaces parallel to the $(111)_{cub}$ plane. The $(111)_{cub}$ faces were mirror polished using a series of diamond pastes down to 3 μm. For the dielectric measurements, the sample was sputtered with gold layers on the $(111)_{cub}$ faces in a central area of 1.5×1.5 mm^2. Two gold wires were attached to the electrodes using silver paste. For the poling of the sample, an electric field of 20 kV cm^{-1} was applied at room temperature and kept on for 30 min. The crystal was then short-circuited to remove possible space charges injected.

X-ray diffraction experiments were carried out on the unpoled crystal using the X22A beamline (32 keV, $\lambda \approx 0.38$ Å, with a penetration depth of about 30 μm at normal incident) from the national synchrotron light source (NSLS) at the Brookhaven National Laboratories. The beamline is equipped with a four-circle Huber diffractometer, with Si(220) and Si(111) analyser-crystals mounted in the diffraction path. The diffraction data were collected at a temperature range between 420 and 25 K upon cooling. The accuracy of the temperature measurement was within ± 5 K and the temperature stability was within ± 2 K. The θ–2θ scans were performed over selected angular ranges centred about the (200), (220) and, in particular, (222) cubic reflections. A least-squares method was used for fitting the diffraction line profiles to different shape functions. In addition to the Gaussian function that describes the proper Bragg peaks at X22A, the Lorentz, pseudo-Voigt and Pearson VII functions were also tested to choose the best one.

Dielectric spectroscopic measurements were performed by means of a computer-controlled system consisting of a Solartron–1260 impedance analyser and a Solartron–1296 dielectric interface, at various frequencies (100 Hz–1 MHz) in the temperature interval between 310 and 620 K. The measurements were carried out under various conditions: (1) zero-field cooling (ZFC); (2) field cooling (FC) for unpoled crystal by applying a dc bias field; (3) zero-field heating (ZFH) for prepoled crystals.

3. Results and analysis

3.1. Structural transformation

Preliminary synchrotron x-ray diffraction experiments were undertaken on a pressed PZN powder sample obtained by crushing small single crystals at beamline X22A in the Bragg–Brentano geometry. The data collected for several characteristic reflections show a single peak for $(200)_{cub}$, a double peak for $(220)_{cub}$ and a double peak for $(222)_{cub}$ reflections, which indicate a non-cubic and very likely a rhombohedral symmetry.

In the $(111)_{cub}$ crystal, the diffraction data around the $(222)_{cub}$ Bragg reflection were carefully measured as a function of temperature. The results obtained at some selected

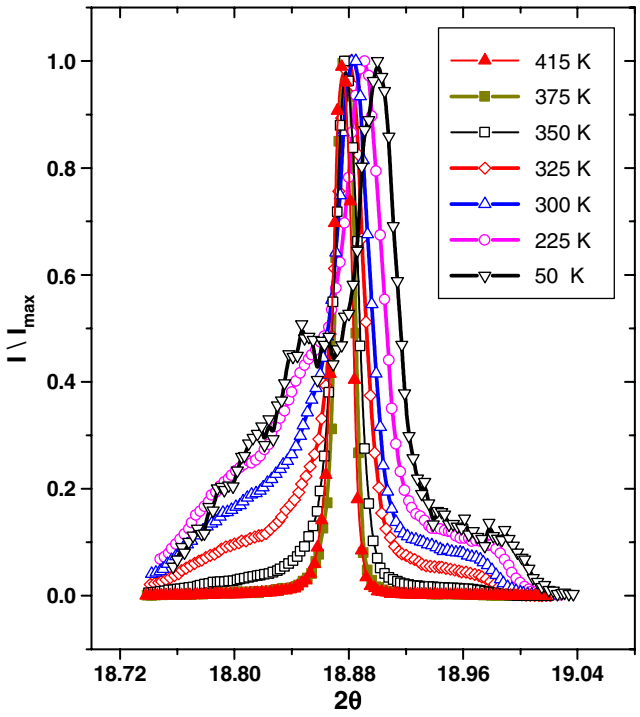

Figure 1. Diffraction pattern around the $(222)_{\mathrm{cub}}$ peak for PZN crystal at selected temperatures between 50 and 415 K (with intensity normalized by I/I_{max}).

temperatures are shown in figure 1 (all diffraction data are intensity normalized by the peak value at each temperature, i.e. I/I_{max}). The peak at 415 K appears sharp and symmetric with an instrument resolution-limited width, indicating the cubic structure (in accord with all previously published results) and the excellent quality of the crystal. On the other hand, the bottom of the peak is slightly broadened, more pronounced at the lower angle side. To visualize this fact better, the profile is shown separately in semi-logarithmic scale in figure 2(a). Such kind of base broadening of x-ray and neutron diffraction peaks in PMN-based relaxors is usually related to the scattering by polar nanoregions [24, 25]. In PZN this effect was also reported in the high-temperature phase, but only for neutron scattering [22]. The full profile can be well fitted by the sum of Gauss and Lorentz functions representing the Bragg and diffuse scattering contributions, respectively. Note that these two functions are centred at slightly different θ values, and the fittings are disturbed at the angles far from the centre.

The spectrum at 390 K (not shown) is almost identical to that of 415 K. But at lower temperatures distinctive shoulders begin to appear from both sides of the peak (figure 1). Upon further cooling, these shoulders become more and more significant and the intensity of the major peak decreases (figure 3), indicating that some regions of the crystal undergo a structural distortion. At low temperatures two peaks expected for the rhombohedral phase are clearly visible, but surprisingly, besides these two peaks, significant shoulders still remain (see figure 2(b)). This means that an additional phase (or phases) not noticed in the previous investigations exists in PZN crystal alongside the rhombohedral phase.

In the temperature interval of 50–325 K the full line profile can be well fitted as a sum of five overlapping Gauss functions. Figure 2(b) demonstrates the fit at 50 K as an example. Two

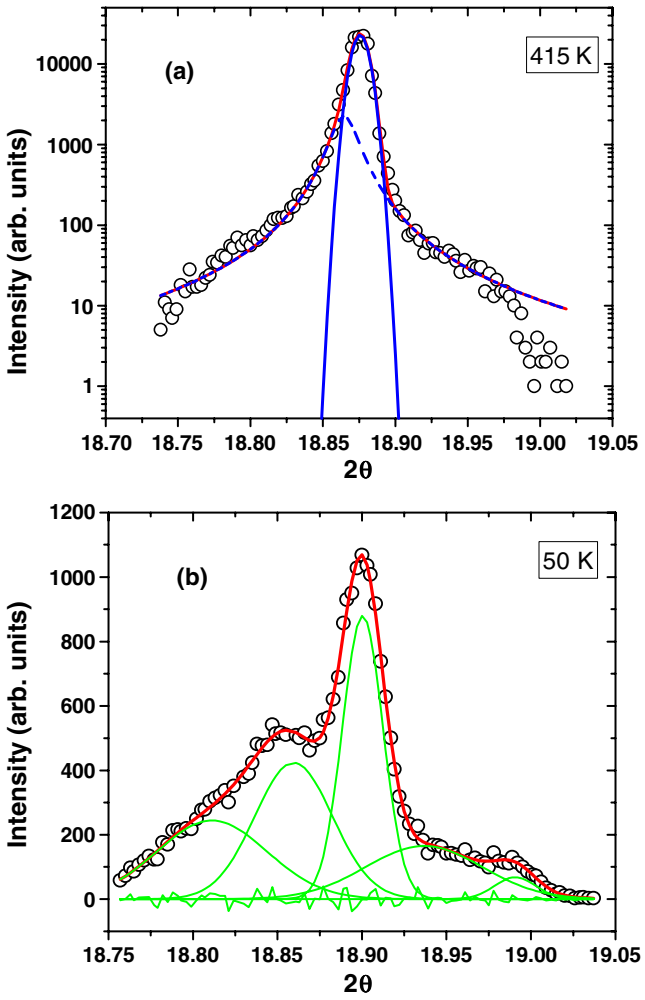

Figure 2. Fitting of the diffraction pattern around the $(222)_{cub}$ peak for PZN crystal at (a) 415 K and (b) 50 K. Circles represent experiment data; Gaussians and Lorentzian used for fitting are represented by solid and broken curves, respectively.

central contributions (i.e. those that give rise to the maxima on the diffraction profile) can be assigned to the rhombohedral phase [$(222)_R$ and $(\bar{2}22)_R$ reflections correspond to low-angle and high-angle maxima, respectively]. The remaining three contributions are related to the other phase of lower (probably a monoclinic or triclinic) symmetry.

The summarized intensity of the peaks related to the new phase (calculated as the sum of intensities of the corresponding fitted peaks) accounts for about 40% of the total intensity of all peaks, which means that this low-symmetry phase exists at a significant concentration. However, the magnitudes of the peaks of this phase are comparatively small for two reasons: (i) the intensity is distributed over more than three peaks, and (ii) the peaks are wider; for example, at 50 K the value of the full width at half maximum (FWHM) is about 0.07° for the two most intense peaks of the new phase, which is much larger than the $(\bar{2}22)_R$ peak (0.024°) and the $(222)_R$ peak (0.046°). The small magnitude of those peaks explains why they can be

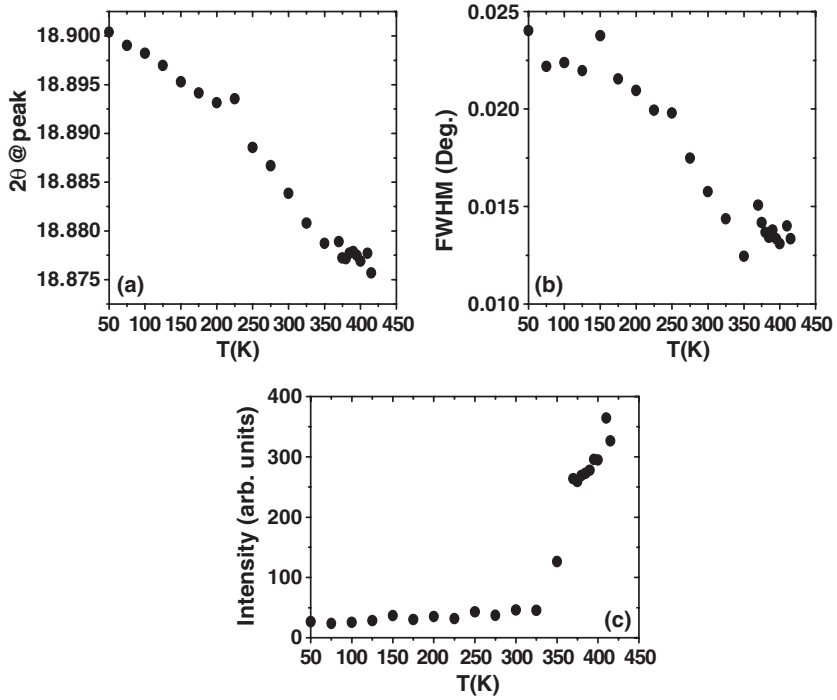

Figure 3. Variations of (a) two-theta (2θ) values, (b) full-width-at-half-maximum (FWHM), and (c) integrated intensity of the major $(222)_{\mathrm{cub}}$ peak as a function of temperature for PZN crystal.

reliably detected only with the help of synchrotron x-ray diffraction having both the intensity and resolution much higher than the conventional x-ray technique.

Note that the central peak, which is single at high temperatures, remains the dominant peak throughout the cooling down to 50 K. Figure 3 shows the variations of the position, FWHM and intensity of this peak as a function of temperature. It can be seen that the FWHM and the angle of the peak position increase upon cooling, first very slowly but much more quickly starting from about 350 K. A sharp drop of peak intensity is also observed between 325 and 370 K, i.e. in the temperature range where the shoulders around the major peak become very pronounced. The line profile cannot be unambiguously fitted in this temperature range. All these features provide evidence for the phase transition. Our results are consistent with the recent study of the (333) and (005) lines of PZN [20], in that the phase transition is diffuse, i.e. in the temperature interval of 325–390 K the cubic phase transforms progressively into the domains of ferroelectric phase so that the different phases coexist in this interval. Indeed, as mentioned above, the distinguishable shoulders around the central peak, signifying the presence of the low-symmetry phase (or phases) were observed already at 385 K. With decreasing temperature these shoulders gradually grow because of the increase of the concentration of the low-symmetry phase. Due to the fact that the lattice plane spacings in the $[111]_{\mathrm{cub}}$ direction are very close in the cubic and rhombohedral phases (i.e. the unit cell changes during the transition in such a way that its dimension in one of the $\langle 111\rangle_{\mathrm{cub}}$ directions remains unchanged) [20], the rhombohedral $(\bar{2}22)_{\mathrm{R}}$ and cubic $(222)_{\mathrm{C}}$ reflections are superimposed and cannot be resolved; that is why only a single peak composed of these two contributions can be observed in the temperature range of the diffuse phase transition. Because of the decrease of the concentration of the cubic phase on cooling, the intensity of this peak decreases (figure 3(c)), and below about 325 K it remains

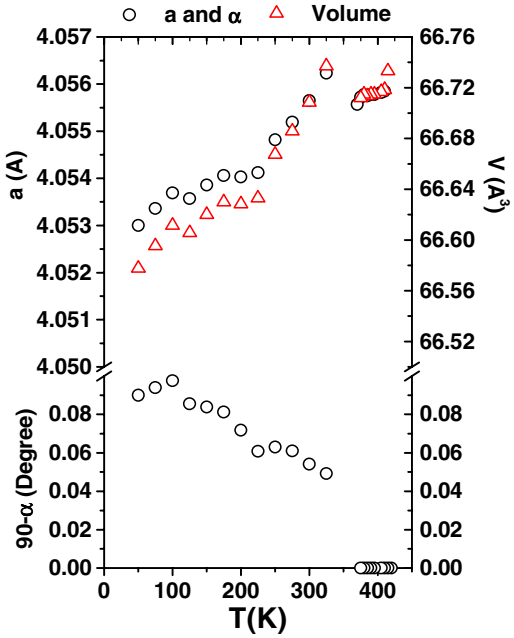

Figure 4. Variations of lattice parameters, a and α, and the unit cell volume, as a function of temperature for the rhombohedral and cubic phases of PZN crystal.

almost temperature independent, which means that the diffuse phase transition is practically completed.

Figure 4 presents the temperature dependences of the lattice parameters a and α and the unit cell volume calculated for the cubic and rhombohedral phases in PZN crystal. The anomaly around 350 K clearly indicates the phase transition. The value of α in the low-temperature $R3m$ phase agrees satisfactorily with that reported for this phase in [20] and is approximately the same value as in the rhombohedral phase of normal perovskite ferroelectrics. Interestingly, the variation of the rhombohedral lattice constant a below the transition temperature (figure 4) shows the same trend as that of PMN [25, 26], reflecting the relaxor behaviour of PZN even in the low-temperature phase(s). The width of the diffraction peaks below the phase transition temperature is much larger than in the high-temperature cubic phase. Figure 3(b) illustrates the FWHM for the major peak. The widths of other peaks are even larger. This effect is usually explained by the small size of ferroelectric domains. The other, probably more important, reason for this in PZN is the internal elastic microstrains caused by the coexistence of different ferroelectric phases. The spontaneous deformations of the parts of the crystal containing different phases are different, which leads to internal stresses and strains. Spontaneous deformation usually increases with decreasing temperature, which is confirmed in our case by the increase of the rhombohedral angle in figure 4. As a result, the FWHM also increases with decreasing temperature (figure 3). Additional line broadening can also arise from a dispersion in lattice parameters, which depends on the distance from the crystal surface [21].

Using the Scherrer equation the size of the ferroelectric domains was estimated from the difference between the squares of the instrumental FHWM and the FHWM observed at 300 K (i.e. at a comparatively high temperature, where the broadening related to internal strains is

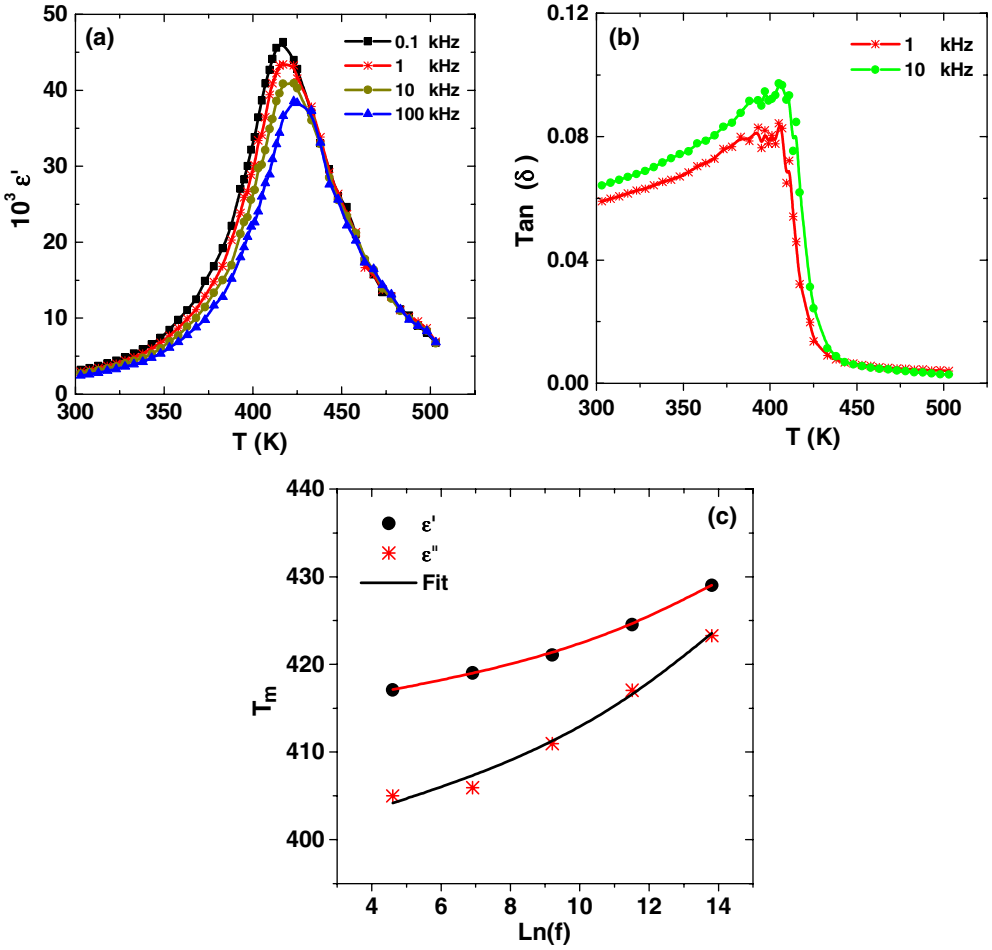

Figure 5. Variations of (a) the real part of dielectric permittivity, and (b) the dissipation factor, as a function of temperature for PZN crystal upon zero-field cooling (ZFC) measured at different frequencies. (c) Frequency dependences of the temperature (T_m) of maximum permittivities (circles for real part and stars for imaginary part) and the fitting (solid curve) to the Vogel–Fulcher relation.

not very large). For the rhombohedral phase we derive a size of ∼70 nm and ∼200 nm from $(222)_R$ and $(\bar{2}22)_R$ peaks, respectively. This means that the domain size in one of the directions (perpendicular to the spontaneous polarization vector) is larger than in the other directions, i.e. the domains have the laminar form. Note that in [20] all the dimensions of rhombohedral domains in PZN were estimated to be the same size (60–70 nm). This discrepancy can be explained by a longer x-ray wavelength used in that work leading to smaller penetration depth (the structure of PZN is known to depend on the distance from crystal surface [21]). The domain size of the new phase is estimated to be in the range 40–80 nm, depending on the direction.

3.2. Dielectric properties

Figures 5(a) and (b) give the variations of the real part of the dielectric permittivity ε' and the dissipation factor $\tan\delta$ as a function of temperature at various frequencies, measured upon

Table 1. Fitting parameters of the Vogel–Fulcher relation for the temperatures of maximum real and imaginary permittivities obtained under different conditions.

	ZFC		FC		ZFH after poling	
	ε'	ε''	ε'	ε''	ε'	ε''
f_0 (Hz)	3e+10	8e+10	5e+10	2e+8	3e+9	5e+11
E_a (K)	263	488	332	165	206	526
T_0 (K)	403	380	393	392	401	377

zero-field cooling (ZFC) for the $(111)_{cub}$ PZN crystal. The strong frequency dispersion of the dielectric constant with the temperature of the maximum, T_m, increasing at higher frequencies, indicates a typical relaxor ferroelectric behaviour. The temperature T_m varies from 417 K at 100 Hz to 429 K at 1 MHz. As in other relaxors, the frequency (f) dependence of T_m can be fitted with the Vogel–Fulcher relation:

$$f = f_0 \exp[-E_a/(T_m - T_0)],$$

where f_0, E_a, and T_0 are the parameters, as shown in figure 5(c). The same fit, but with a different set of parameters, can be applied to the frequency and temperature dependences of the imaginary permittivity maximum (not shown). The best-fit results are presented in table 1. It is worth noting that below T_m no evidence of the structural phase transition, which was detected between 390 and 325 K in the above-mentioned x-ray diffraction experiments, can be observed in the dielectric properties.

Figure 6(a) shows the temperature dependence of the real permittivity of the unpoled crystal measured at various frequencies upon cooling under a dc bias field of 1.2 kV cm^{-1} (FC). The strong dispersion due to relaxor relaxation around T_m remains. However, at $T_C \approx 390$ K, the dielectric constant undergoes a discontinuous change in slope with the values at different frequencies merging together and dropping sharply. Below T_C the frequency dispersion is attenuated dramatically. The dielectric relaxation around T_m can also be fitted with the Vogel–Fulcher relation for both the real and imaginary parts of the permittivity, with the fitting parameters given in table 1.

Figure 6(b) presents the temperature and frequency dependences of the dielectric constant of the PZN crystal prepoled at room temperature (at 20 kV cm^{-1}), which were measured upon zero-field heating (ZFH) after poling. In the low-temperature range, the permittivity is almost non-dispersive. Upon further heating, a sharp peak of dielectric constant occurs at $T_C = 388$ K. Above T_C, the strong dielectric dispersion, characteristic of relaxor relaxation, reappears, suggesting that the PZN crystal reenters the relaxor state. The transition temperature T_C does not depend on frequency, as opposed to the behaviour of T_m. The frequency dependence of the latter can also be well fitted into the Vogel–Fulcher law with the fitting constants provided in table 1.

It is interesting to note that

(i) above T_C the electric field has almost no effect on the dielectric relaxation behaviour around T_m, which can be fitted into the Vogel–Fulcher relation with fitting parameters only slightly different from those of ZFC, and

(ii) the sharp anomalies of the dielectric constant upon ZFH after poling and upon FC are observed at approximately the same temperature as $T_C \approx 390$, where the diffuse phase transition begins upon ZFC, as revealed by synchrotron x-ray diffraction experiments.

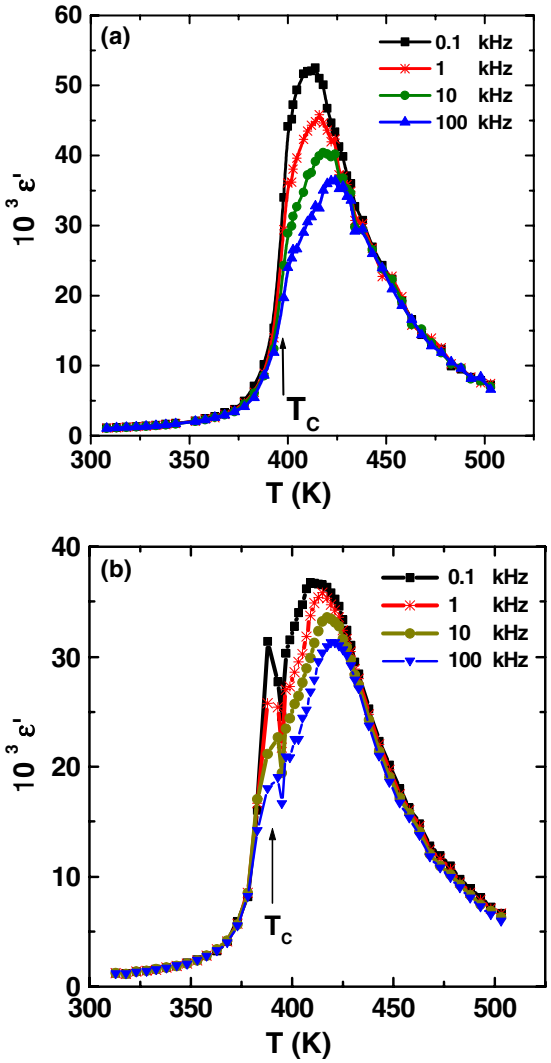

Figure 6. Variation of the real part of the dielectric permittivity measured at different frequencies as a function of temperature for PZN crystal upon (a) cooling under a field of 1.2 kV cm^{-1} (FC), and (b) zero field heating (ZFH) after poling at room temperature.

4. Discussion

Let us discuss the structure and properties of the PZN crystals studied in this work by comparing them with the well-documented structure and properties of the prototypical relaxor ferroelectric PMN (see e.g. [1]). The temperature and frequency dependences of the dielectric permittivity look very similar in both crystals, with observed broad and high $\varepsilon(T)$ peak and strong dispersion causing the Vogel–Fulcher-type shift of T_{m} with frequency (see figure 5). In both crystals additional anomalies in the temperature dependences of permittivity and losses that are initially absent at zero field can be induced by applying a strong enough electric field (see figure 6). In both cases, the high-temperature slope of the diffuse permittivity peak can be scaled by

the Lorenz-type quadratic function with close values of the diffuseness parameter ($\delta = 28$ K for PZN and $\delta = 41$ K for PMN), as described in detail in [27] (the data used for scaling came from the same PZN crystal as in this work). The structures of PMN and PZN at high temperatures (around T_m and above) are also similar. It is usually believed that in PMN the structure is macroscopically cubic with nanometric inclusions of polar order. In PZN the existence of PNRs has recently been deduced from neutron scattering experiments in [22] and confirmed in the present work by the observed broadening of the base of the diffraction peak. On the other hand, the low-temperature structures of these two materials are quite different. In PMN the x-ray and neutron diffraction investigations do not indicate any macroscopic distortion of the cubic lattice. PZN, in contrast, exhibits a reduction of symmetry below about 350 K where we observed the splitting of (222) lines. Two central contributions (peaks) can be attributed to the rhombohedral phase, which was also observed in previous investigations (e.g. in [20]). In addition, we have revealed the presence of another low-symmetry phase with a significant concentration which was not reported before (the present data do not allow us to determine the symmetry and the type (ferroelectric or antiferroelectric) of this new phase; such an investigation is underway). We also confirmed that the phase transition in PZN is diffuse, i.e. the high-temperature cubic phase and the low-temperature phases coexist in a temperature interval of several dozens of degrees.

Note that the studies of the PZN crystal with the help of neutron and high-energy (67 keV) x-ray diffraction revealed a different low-temperature phase (the so-called X-phase) but not the rhombohedral one [21, 22, 28]. The X-phase exhibits a cubic unit cell. It was not observed in this work, nor was it in other works in which low-energy x-rays were used. This discrepancy can be explained [21] by the small penetration capability of low-energy radiation, so that it probes only the parts of the crystal not far from the surface ('skin'). X-phase seems to be located in the bulk and can be detected only by high-energy radiation. As the phase content depends on the distance from the crystal surface (X-phase inside, 'normal' phases at the surface), one can suspect that the rhombohedral phase and the additional low-symmetry phase discovered in this work are also separated in space. Further experiments are needed to determine if these two phases are mixed homogeneously or exist separately.

The important point to underline here is that the PNR-related diffuse scattering giving rise to the tails around the sharp $(222)_{cub}$ Bragg peak at high temperatures has been observed in our x-ray diffraction experiments. This means that PNRs exist not only in the crystal bulk, transforming to the X-phase upon cooling, but also in the 'skin' of the crystal which undergoes a transition into phases with normal ferroelectric distortion.

It is interesting to compare the behaviour of PZN with those of other perovskite materials which exhibit a spontaneous relaxor to normal ferroelectric phase transition (e.g. $Pb(Fe_{1/2}Nb_{1/2})O_3$ [29], $Pb(Sc_{1/2}Nb_{1/2})O_3$ [30], or $Pb(Mg_{1/3}Nb_{2/3})O_3$–$PbTiO_3$ solid solutions with high concentration of $PbTiO_3$). In these crystals the characteristic diffuse $\varepsilon(T)$ peak exhibiting Vogel–Fulcher frequency dependence is accompanied by a dielectric anomaly at several degrees below T_m. This anomaly is related to the spontaneous (i.e. without external field) transition to the ferroelectric phase upon cooling and it can be very sharp. Below the phase transition temperature a well-defined ferroelectric phase exists with macroscopic domains of ~ 1 μm in size.

One can see that the behaviour of the PZN crystals sits in an intermediate position between the behaviour of prototypical relaxor PMN and that of the crystals with a sharp spontaneous relaxor to normal ferroelectric phase transition. A spontaneous transition to the ferroelectric phase is observed in PZN, but this transition is diffuse and thus it is not associated with the sharp dielectric anomalies. The size of the ferroelectric domains is considerably smaller than the size of normal ferroelectric domains, but larger than the size of polar nanoregions in PMN.

Furthermore, the ferroelectric state in PZN exists in the outer layers only. The inner part remains at low temperature in the cubic phase which is similar to the low-temperature phase of PMN [22].

To interpret our results we apply the kinetic model of phase transitions, which is developed to describe the diffuse and sharp phase transitions in compositionally disordered crystals [31]. According to this model the PNRs begin to appear within the paraelectric phase at $T_d \gg T_{0m}$ (T_{0m} is the average temperature of the ferroelectric phase transition) as a result of local 'phase transitions' caused by compositional inhomogeneities in the disordered crystal (the nature of these inhomogeneities and the peculiarities of polar order inside the PNRs are discussed in [32] and [13]). The equilibrium size and number of PNRs gradually increase during cooling. At a certain lower temperature T_C the PNRs become metastable and their sudden growth is possible (similar to the isothermal growth of the nuclei of a new phase in the case of the normal first-order phase transition). The model parameter ρ_c (which is directly proportional to T_{0m} and inversely proportional to the diffuseness of the phase transition) determines the fraction of crystal bulk filled with PNRs at $T = T_C$. If ρ_c is comparatively small, the concentration of PNRs at T_C is large and the growth of any PNR is limited by the neighbouring PNRs as well as by the areas having a lower local Curie temperature. To form a large polar domain in some regions, PNRs have to merge, i.e. the directions of their dipole moments have to change to be the same for all PNRs in this region. But the reorientation of all PNRs appears to be impossible because at least some of them are frozen. This freezing can be due to one of the following reasons:

(i) the temperature is too low to activate the PNRs so as to overcome the potential barrier between the states with different directions of PNR dipole moment,
(ii) a dipolar glass state is formed in which the directions of PNR moments are fixed by the frustrated interactions between them, and
(iii) PNR moments are pinned by local random electric and/or elastic fields.

Consequently the size and number of PNRs remain almost unchanged when the crystal passes through T_C. As a result, the long-range polar order characteristic of the ferroelectric state cannot develop and thereby no noticeable anomalies of structural parameters and dielectric (and other physical) properties can be observed. This scenario seems to be valid for PMN in which PNRs are commonly believed to exist at all temperatures below T_d and all the three reasons mentioned above for their freezing can be expected. In PZN the ρ_c parameter is larger due to a higher T_{0m} and a smaller (see above) phase transition diffuseness δ. A larger ρ_c means that at T_C the concentration of PNRs is smaller (the distance between them is rather large) and they have room to grow up to mesoscopic sizes large enough to be detected by x-ray and neutron diffractions. The higher transition temperature in PZN probably facilitates the formation of the larger polar regions in another way. At a higher temperature the dipole moments of some PNRs can be reoriented by thermal motion. Consequently the growth of PNRs at T_C is accompanied by the reorientation of some of the neighbouring PNRs so that several PNRs can merge to form larger ferroelectric domains (the merging decreases the energy related to the domain walls). Upon further cooling below T_C the process of domain formation goes on because of the increase in ferroelectric distortion and the transformation to the ferroelectric phase of the regions with reduced local Curie temperature. This process has been revealed in the diffraction experiments. The corresponding anomalies (figure 3) are observed not at a well-defined temperature, but smeared over a wide temperature interval.

Materials with a sharp transition from relaxor to normal ferroelectric state are usually characterized by a small diffuseness parameter δ and consequently a large ρ_c parameter. As

a result, the concentration of PNRs is small at T_C and they are free to grow into macroscopic ferroelectric domains.

The dielectric behaviour of relaxors is also determined by the kinetics of the formation and evolution of the PNRs and ferroelectric domains. This is because the dielectric response of relaxors in the temperature range around T_m arises mainly from the relaxation of PNRs and their boundaries, rather than from the non-relaxation ionic polarization related to the relative displacement of the positive and negative sublattices, as in the case of normal displacive ferroelectrics (see e.g. [33] for more detailed discussion). In the relaxors that do not undergo a transition into the ferroelectric phase upon cooling (e.g. in PMN) the temperature evolution of PNRs occurs without abrupt changes in their size and concentration, and consequently there are no sharp anomalies in the temperature dependences of the permittivity. The relaxors with a sharp spontaneous phase transition into the normal ferroelectric phase show an abrupt drop of dielectric constant at T_C due to the transformation of PNRs into macroscopic ferroelectric domains at this temperature. In the intermediate case of PZN, the transformation of PNRs into ferroelectric domains takes place gradually so that the dielectric permittivity changes without sharp anomalies. The behaviour of PZN crystals is also complicated by the presence of the bulk X-phase. The dielectric properties of pure X-phase are not definitely known, but structural investigations of inner parts of the crystal did not reveal any sharp anomalies in the temperature range where the transition in outer layers is observed (325–390 K), thus the dielectric anomalies in this range should not be expected either. The region of X-phase being connected in series to the outer layers of 'normal' ferroelectric phase can lead to an additional decrease of the diffuse dielectric anomaly at T_C so that it becomes unnoticeable. At temperatures above the diffuse phase transition (including T_m) the structure of the inner and outer parts of the crystal seems to be qualitatively the same, and the permittivity is determined by the relaxation of PNRs. At temperatures below the transition the main contribution to the dispersion comes from the relaxation of the walls between mesoscopic domains existing in outer layers and PNRs which remain in the X-phase.

An electric field applied on the PZN crystal upon cooling is able to reorient PNRs, so that all of them have the same (or almost the same) orientations of dipole moments, and at T_C, where the process of intensive growth of PNRs begins, they can easily merge to form macroscopic ferroelectric domains. It is known that these macroscopic domains appear under the field not only at the surface, but also in the bulk of the crystal [21]. The number of relaxing elements (e.g. domain walls and boundaries between different phases) that are able to contribute to the dielectric constant decreases rapidly during this process, leading to the distinct dielectric anomaly at T_C. Below T_C, the dielectric dispersion is almost suppressed (figure 6(a)). Upon heating of the poled crystal, the phase transition occurs at T_C accompanied by the sharp dielectric peak (figure 6(b)), indicating that the crystal transforms back to the same relaxor state with the presence of PNRs as it was in the zero-field experiments. As a result, the Vogel–Fulcher parameters remain almost unchanged (see table 1). However, in contrast to the zero-field experiments, the orientations of PNRs are no longer random. Instead, the PNRs subsystem is poled (or partially poled) so that the magnitude of the permittivity is different (smaller).

It should be pointed out that the phenomenological kinetic model discussed above does not take into account the possible symmetry of the ferroelectric phase. For such a consideration, the 'soft polar nanoregions' model [13] can be applied. It is argued in this model that due to the randomness of microscopic forces responsible for the onset of spontaneous polarization, each PNR consists of differently polarized unit cells. This model implies that the local symmetry of the structure inside the PNR can randomly vary in space and probably with time. We believe that different local symmetry prevails in different PNRs so that they can develop upon cooling

into the ferroelectric domains of different symmetry. As a result at least two phases are present in PZN at low temperatures.

5. Conclusions

We have shown in this study that the $Pb(Zn_{1/3}Nb_{2/3})O_3$ crystal is a unique example of a relaxor in which, in contrast to the classical relaxor PMN, a spontaneous (i.e. without external electric field) ferroelectric phase transition occurs, but, in contrast to some other relaxors exhibiting sharp spontaneous transition to a ferroelectric phase (e.g. $Pb(Fe_{1/2}Nb_{1/2})O_3$), this transition is diffuse and observed only near the surface of the crystal. As detected by high-resolution synchrotron x-ray diffraction in the absence of an electric field, PZN crystal undergoes a diffuse structural transformation from the high-temperature state, which is macroscopically cubic and contains polar nanoregions typical of relaxors, to the low-temperature state composed of mesoscopic (40–200 nm) domains of the rhombohedral ferroelectric phase and a second phase with lower symmetry. On cooling, the domains of these low-temperature phases begin to appear at $T_C \approx 390$ K and grow progressively at the expense of the cubic phase. Below $T \approx 325$ K the cubic phase is no longer observable. The so-called X-phase, recently discovered in the central (bulk) parts of PZN crystal with the help of high-energy x-ray and neutron diffraction, was not observed in the present work because the x-ray energy used (32 keV) was not high enough to penetrate deeply into the crystal.

The dielectric properties show typical relaxor ferroelectric behaviour with a broad and dispersive peak of dielectric constant at $T_m \approx 415\ K > T_C$, which can be fitted into the Vogel–Fulcher relation, while no clear anomalies in dielectric properties can be associated with the structural phase transformation at $\sim T_C$. Application of an electric field (1.2 kV cm^{-1}) upon cooling induces a comparatively sharp phase transition at $T_C \approx 390$ K with the establishment of the ferroelectric phase with macroscopic domains, as revealed by the anomaly in the temperature dependence of the dielectric constant at T_C and the disappearance of significant dielectric dispersion below T_C. The state induced upon field cooling collapses under ZFH at T_C in the form of a sharp phase transition with the breaking down of the macro polar domains back into the relaxor state. The relaxor behaviour is fully recovered with typical relaxor dielectric relaxation around $T_m \approx 415$ K and the same fitting parameters to the Vogel–Fulcher relation.

The structural behaviour, dielectric properties and phase transition of the PZN crystal are discussed in the light of the kinetic model of phase transitions in disordered crystals and the model of 'soft nanoregions' in relaxors.

Acknowledgments

The authors thank W Chen for help in crystal preparation, and G Xu, Z Zhong and C Stock for useful discussion. This research was supported by the Natural Sciences and Engineering Research Council of Canada (NSERC), the US Office of Naval Research (Grant No. N00014-99-1-0738) and the US DOE (Contract No. DE-AC02-98CH10886).

References

[1] See, for a review,
Cross L E 1994 *Ferroelectrics* **151** 305
Ye Z-G 1998 *Key Eng. Mater.* **155/156** 81
Bokov A A 1992 *Ferroelectrics* **131** 49
[2] Park S E and Shrout T R 1997 *J. Appl. Phys.* **82** 1804

[3] See, for a review,
Park S-E and Hackenberger W 2002 *Curr. Opin. Solid State Mater. Sci.* **6** 11
Bellaiche L 2002 *Curr. Opin. Solid State Mater. Sci.* **6** 19
Noheda B 2002 *Curr. Opin. Solid State Mater. Sci.* **6** 27
Ye Z-G 2002 *Curr. Opin. Solid State Mater. Sci.* **6** 35
[4] Gehring P M, Wakimoto S, Ye Z-G and Shirane G 2001 *Phys. Rev. Lett.* **87** 277601
[5] Wakimoto S, Stock C, Birgeneau R J, Ye Z-G, Chen W, Buyers W J L, Gehring P M and Shirane G 2002 *Phys. Rev.* B **65** 172105
[6] Ye Z-G and Schmid H 1993 *Ferroelectrics* **145** 83
[7] Tu C-S, Schmidt V H and Siny I G 1995 *J. Appl. Phys.* **78** 5665
[8] Hirota K, Ye Z-G, Wakimoto S, Gehring P and Shirane G 2002 *Phys. Rev.* B **65** 104105
[9] Ye Z-G 1995 *Ferroelectrics* **172** 19–30
[10] Calvarin G, Husson E and Ye Z-G 1995 *Ferroelectrics* **165** 349
[11] Bokov A A and Ye Z-G 2000 *J. Phys.: Condens. Matter* **12** L541
[12] Bokov A A and Ye Z-G 2002 *Phys. Rev.* B **65** 144112
[13] Bokov A A and Ye Z-G 2002 *Phys. Rev.* B **66** 064103
[14] Blinc R, Dolinsek J, Gregorovic A, Zalar B, Filipic C, Kutnjak Z, Levstik A and Pirc R 1999 *Phys. Rev. Lett.* **83** 424
[15] Pirc R and Blinc R 1999 *Phys. Rev.* B **60** 13470
[16] Smolenskii G A, Krainik N N, Berezhnoi A A and Myl'nikova I E 1969 *Sov. Phys.—Solid State* **10** 2105
[17] Yokomizo Y, Takahashi T and Nomura S 1970 *J. Phys. Soc. Japan* **28** 1278
[18] Nomura S, Endo M and Kojima F 1974 *Japan. J. Appl. Phys.* **13** 2004
[19] Ye Z-G, Dong M and Zhang L 1999 *Ferroelectrics* **229** 223
[20] Lebon A, Dammak H, Galvarin G and Ould Ahmedou I 2002 *J. Phys.: Condens. Matter* **14** 7035
[21] Xu G, Zhong Z, Bing Y, Ye Z-G, Stock C and Shirane G 2003 *Phys. Rev.* B **67** 104102
[22] Stock C, Birgeneau R J, Wakimoto S, Gardner J S, Chen W, Ye Z-G and Shirane G 2004 *Phys. Rev.* B **69** 094104
[23] Zhang L, Dong M and Ye Z-G 2000 *Mater. Sci. Eng.* B **78** 96
[24] Bonneau P, Garnier P, Calvarin G, Husson H, Gavarri J R, Hewat A W and Morell A 1991 *J. Solid State Chem.* **91** 350
[25] Ye Z-G, Bing Y, Gao J, Bokov A A, Noheda B and Shirane G 2003 *Phys. Rev.* B **67** 104104
[26] Dkhil B, Kiat J M, Calvarin G, Baldinozzi G, Vakhrushev S B and Suard E 2002 *Phys. Rev.* B **65** 024104
[27] Bokov A A, Bing Y-H, Chen W, Ye Z-G, Bogatina S A, Raevski I P, Raevskaya S I and Sahkar E V 2003 *Phys. Rev.* B **68** 052102
[28] Xu G, Zhong Z, Bing Y, Ye Z-G, Stock C and Shirane G 2004 *Phys. Rev.* B **70** 064107
[29] Bokov A A and Emeliyanov S M 1991 *Phys. Status Solidi* b **164** K109
[30] Chu F, Reaney I M and Setter N 1995 *J. Appl. Phys.* **77** 1671
[31] Bokov A A 1994 *Phys. Solid State* **36** 19
Bokov A A 1997 *Ferroelectrics* **190** 197
[32] Bokov A A 1997 *JEPT* **84** 994
Bokov A A 1994 *Solid State Commun.* **90** 687
[33] Ye Z-G and Bokov A A 2004 *Ferroelectrics* **302** 473